Pressure-induced structural transformations in the Mott insulator FeI_2

G. Kh. Rozenberg, M. P. Pasternak, and W. M. Xu
School of Physics and Astronomy, Tel-Aviv University, Ramat-Aviv 69978, Tel Aviv, Israel

L. S. Dubrovinsky
Bayerisches Geoinstitut, University Bayreuth, D-95440 Bayreuth, Germany

J. M. Osorio Guillén, R. Ahuja, and B. Johansson
Condensed Matter Theory Group, Department of Physics, 751 21 Uppsala, Sweden

T. Le Bihan
European Synchrotron Radiation Facility, BP 220, 38043 Grenoble Cedex, France
(Received 1 July 2002; revised manuscript received 24 October 2002; published 7 August 2003)

A full-profile refinement of the layered antiferromagnetic FeI_2 crystallographic structures at pressures up to 70 GPa were performed combined with *ab initio* calculations to particularly elucidate the structural aspects of the recently observed pressure-induced quenching of the orbital term of the Fe^{2+} moment and of the Mott transition. Synchrotron powder XRD diffraction studies have shown that at ~17 GPa a substantial alteration of the lattice parameters takes place which is attributed to the quenching of the orbital term. Starting at $P \sim 20$ GPa and completed at ~35 GPa, a sluggish structural phase transition takes place which can be attributed to the onset of a Mott transition as has been previously observed by resistance and MS studies. In agreement with *ab initio* calculations, the doubling of lattice parameters and the formation of a new Fe sublattice replacing the original CdI_2-type structure, can explain this structural transition. The latter alterations in the Fe sublattice may indicate a trend of the Fe sites to disorder in the new high pressure phase. This first-order phase transition is characterized by a significant change of the unit cell parameters, a reduction in volume, and a change of the Fe-I distances. The substantial reduction of the Fe-I distances with minimal changes in the Fe-Fe bond lengths at the transition, suggests a charge-transfer-type gap closure mechanism involving the I*p*-Fe*d* bands. At $P > 40$ GPa a overturn of the structural transition is observed resulting in the return of the original, CdI_2-type structure.

DOI: 10.1103/PhysRevB.68.064105 PACS number(s): 61.50.Ks, 62.50.+p, 61.10.−i, 71.30.+h

I. INTRODUCTION

During the last decade we witnessed a considerable progress in the studies Mott insulators phenomena in transition-metal (TM) compounds in which the process of pressure-induced Mott-transition occurs, namely, the strongly correlated *d*-electrons systems transform into a normal metallic state.[1] This was achieved by numerous high-pressure (HP) studies of ferrous and ferric compounds applying Mössbauer spectroscopy (MS), the only method for magnetic studies at very high pressures,[2] combined with electrical resistivity for probing of transport properties.[3] In spite of these spectroscopy and resistance studies the effect of correlation breakdown on structural features remained unresolved. *A priori*, the Mott-Hubbard (MH) gap closure and its associated consequences such as insulator-metal transition and collapse of the TM moments does not necessarily imply a structural change. A pressure-induced Mott transition (MT) was reported in the layered antiferromagnetic NiI_2 (Ref. 4) and later in CoI_2.[5] It was shown that under pressure NiI_2 undergoes a concurrent insulator-metal transition into a normal metal with magnetism collapse at exactly the same pressure (19 GPa). It was found that within the experimental errors the transition is isostructural and practically isochoric. However, from the few crystallography studies following temperature-induced Mott transition in $RNiO_3$ (R=Pr, Nd, Eu, Sm),[6] V_2O_3, and Cr_2O_3-V_2O_3 (Ref. 7) it was found that an appreciable changes of the interatomic distances *do* take place which might result into crystallographic symmetry modifications due to strong distortion.[7] A recent structural study of pressure-induced Mott transition in Fe_2O_3 (Ref. 8) clearly showed that the structural alterations and a 10% drop in the molar volume coincided with a MT, sic, an electronic transition.

Another pressure-induced electronic feature discovered recently is the quenching of the orbital ordering in $LaMnO_3$.[9] It was shown that orbital order is being suppressed at $P > 18$ GPa and only at 32 GPa a MT took place. Possibly related to this high-pressure feature was the recent finding of pressure-induced quenching of the Fe^{2+} magnetic-moment *orbital* term in FeI_2 by Pasternak *et al.*[10] observed by ^{57}Fe Mössbauer spectroscopy. The orbital quenching was explained as due to an increase in the crystal-field, ensuring also the breakdown of the spin-orbit coupling which resulted in reorientation of the magnetic moment.

In this paper we present a detailed high pressure crystallographic study of the layered antiferromagnetic, Mott insulator FeI_2 [space group $C\bar{3}m$ (Ref. 11)]. A full-profile refinement of the FeI_2 crystallographic structures, up to 70 GPa, based on extensive powder synchrotron XRD diffraction data combined with *ab initio* calculations will be documented.

The work's objective was to elucidate the structural aspects as a result of the (i) quenching of the orbital term at 17 GPa and (ii) the onset of the Mott transition at ~20 GPa. As will be shown, this work will add new aspects to high pressure structural phase transformations resulted from or induced by electronic transition in TM ions.

II. METHODS

Experimental. FeI_2 was synthesized by direct reaction in vacuum of spectroscopic pure iodine vapor and metallic iron at 500 °C in an evacuated quartz tube.[12] Due to the hygroscopic nature of FeI_2 the samples were loaded into the TAU miniature opposing-plates DAC's (Ref. 13) in a glove box under exceptionally dry conditions. The sample was loaded into a cavity of 100 μm in diameter and 30–40 μm thickness drilled in 301-SS gaskets. Argon was used as a pressurizing medium. The sample quality was determined by MS and XRD. HP-XRD studies were performed up to 70 GPa in the angle-dispersive mode at the ID30 beam line of the European Synchrotron Radiation Facility, Grenoble. Three slots of measurements were performed at $\lambda = 0.4246$, 0.36503, and 0.3644 Å wavelength. Diffraction images were collected using image plates with exposure times of ~5 min. The image data were integrated using the FIT2D program[14] and the resulting diffraction patterns were analyzed with the GSAS (Ref. 15) program. The uncertainties in the lattice parameters reported in Tables I and II are from the GSAS fitting output. Pressure was measured using the ruby fluorescence technique and Au marker.

The ab initio calculations. Total energy calculations were performed using the full-potential linear muffin-tin-orbital (FP-LMTO) method[16] based on the generalized-gradient approximation (GGA). The PBE parametrization for the exchange and correlation potential was employed.[17] Basis functions, electron densities, and potentials were calculated without any geometrical approximation.[16] These quantities were expanded in combinations of spherical harmonic functions with a cutoff at $l = 8$, inside nonoverlapping spheres surrounding the atomic sites (muffin-tin spheres), and in a Fourier series in the interstitial region. The muffin-tin spheres (MFT's) occupied approximately 65% of the unit cell. The radial parts of the basis functions inside the MFT's were calculated from a wave equation for the $l = 0$ component of the potential inside the spheres that included mass velocity, Darwin, and higher-order corrections, but not spin-orbit coupling. Spin-orbit coupling and the higher l components of the potential in the MFT's and all of the Fourier components of the potential in the interstitial region were included in the crystal Hamiltonian.[18] The radial basis functions within the MFT's, calculated as described above, are linear combinations of radial wave functions and their energy derivatives computed at energies appropriate to their sites, with principal as well as orbital atomic quantum numbers. Outside the MFT's the basis functions were combinations of spherical Neumann or Hankel functions.[19,20] In the present calculations we made use of pseudocore $3p$ and $4d$ states for Fe and I, respectively; and valence band $4s$, $4p$, and $3d$ basis functions for Fe, and valence band $5s$, $5p$, and $5d$ basis functions for I, with corresponding two sets of energy parameters: one appropriate for the semicore $3p$ and $4d$ states and the other for the valence states. The resulting basis formed a single, fully hybridizing basis set. This approach had been previously confirmed to give a well-converged basis.[16]

TABLE I. The refined structural parameters of CdI_2-type phases of FeI_2 at various pressures.

Pressure (GPa)	a (Å)	c (Å)	u	c/a
LP phase				
0 (Ref. 15)	4.04	6.75	0.25	1.6708
2.7	3.9514(4)	6.3717(21)	0.265(2)	1.6125
4	3.9264(2)	6.2486(3)	0.254(2)	1.5917
6.95	3.8775(17)	6.025(8)	0.260(3)	1.5538
7.8	3.8551(5)	6.057(5)	0.275(2)	1.5712
10.3	3.8232(3)	5.999(6)	0.277(4)	1.5692
12.5	3.7882(4)	5.919(4)	0.282(2)	1.5625
13.6	3.7646(4)	5.929(6)	0.282(2)	1.5749
14.2	3.7458(16)	5.939(11)	0.273(5)	1.5855
16.9	3.671(14)	5.842(34)	0.286(5)	1.5913
19.4	3.5989(1)	5.720(6)	0.281(4)	1.5898
IP phase				
16.9	3.587(30)	5.986(27)	0.274(4)	1.6685
19.4	3.551(9)	5.960(47)	0.2951(17)	1.6789
20.6	3.5410(18)	5.882(6)	0.268(5)	1.6611
23.2	3.538(3)	5.887(14)	0.249(4)	1.6639
25.8	3.529(5)	5.832(18)	0.275(4)	1.6526
27.5	3.521(4)	5.802(19)	0.222(3)	1.6478
HP phase				
40.3	3.5372(6)	4.995(6)	0.2937(18)	1.4121
49.1	3.5428(17)	4.765(6)	0.286(6)	1.345
58.8	3.4960(2)	4.651(5)	0.286(2)	1.3304
69	3.4809(13)	4.581(9)	0.289(2)	1.316

For sampling the irreducible wedge of the Brillouin zone we used the special **k**-point method,[21] with 193 **k** points for FeI_2 in the CdI_2 type structure and 65 **k** points in the big cell model structure. In addition to using the special **k**-point technique we have, in order to speed up the convergence of the **k**-point sampling, associated each calculated eigenvalue with a Gaussian broadening of width 20 mRy.

A complete optimization of the geometry (ionic coordinates and c/a ratio) has been done, using the Hellmann-Feynman forces on the ions for each calculated volume and c/a value. The calculations described above were done for the ferromagnetic state of both structures, in spite of the ground state at ambient pressure of FeI_2 in the CdI_2 type structure is an antiferromagnetic one. This is justified because the magnetic ordering of FeI_2 is very complex and the calculations become rather complicated, furthermore, we do not know how is the magnetic ordering in the big cell model structure proposed here. However, we are more focused to phase stabilities than ground state properties, and the total

TABLE II. The refined structural parameters of the HP phase (BC type) at various pressures. For the meaning of the internal parameters see Ref. 23.

Pressure (GPa)	a (Å)	c (Å)	$I_{3(x)}$	$I_{3(z)}$	$I_{4(x)}$	$I_{4(z)}$	c/a
20.6	7.261(2)	10.639(5)	0.165	0.126	0.170	0.625	1.4652
23.2	7.1966(18)	10.744(10)	0.166	0.125	0.170	0.626	1.4929
25.8	7.1940(19)	10.668(10)	0.162	0.124	0.172	0.625	1.4829
27.5	7.1997(11)	10.404(6)	0.164	0.134	0.172	0.625	1.4451
30.9	7.1240(12)	10.284(8)	0.168	0.136	0.173	0.628	1.4436
32.3	7.1481(9)	10.136(4)	0.171	0.140	0.173	0.631	1.418
35.3	7.1160(12)	10.080(10)	0.173	0.142	0.176	0.629	1.4165

energy comparison of the ferromagnetic solutions for both structures is assumed to be satisfactory for this study.

III. RESULTS

Ferrous di-iodide crystallizes in the hexagonal CdI_2-type structure.[11] The low-pressure phase can be viewed as a hexagonal close packing arrangement of iodine ions with the small ferrous ions nested between planes of the iodides (intralayer I-Fe-I). Each Fe atom has an octahedral arrangement of iodine nearest neighbors and sheets of iron ions are separated by two layers of iodine (interlayer I-I) as can be seen in Fig. 1(a). This structure can be completely characterized in a hexagonal setting by the two lattice parameters a and c, the iron position (0,0,0), and the iodine position $\pm(1/3,2/3,u)$. Those parameters have been refined from the powder XRD data at pressures to 20 GPa. Typical diffraction patterns recorded in the 0-32 GPa pressure range are shown in Fig. 2.

The low pressure phase. Up to 17 GPa, designated as the low pressure phase (LP), the experimental diffraction patterns could be satisfactorily fitted with the CdI_2 structure [see Fig. 3(a)] with w_{Rp} being less than 1.9% and Rp less than 1.2%. Parameters c, a, and the volume decreasing continuously by ~ 14, ~ 9, and $\sim 27\,\%$, respectively, at this pressure range [see Figs. 4(a), 4(b)]. The numerical results of the refinement are summarized in Table I. Note that the iodine coordinate u shows a clear trend to increase with pressure. The c/a value decreases monotonically with pressure due to the soft anisotropic compression along the c axis, from 1.67 to a minimum of 1.57 at ~ 10 GPa, followed by a slight increase to 1.59 at 15 GPa [see inset in Fig. 4(a)]. The data for the molar volume as a function of pressure were fitted using the Birch-Murnaghan (BM) equation of state[22]

$$P = 1.5K_0[(V_0/V)^{7/3} - (V_0/V)^{5/3}] \times [1 - 0.75(4 - K_0')\{(V_0/V)^{2/3} - 1\}], \quad (1)$$

where K_0, K_0', and V_0 are the bulk modulus, its pressure derivative, and the unit cell volume at 1 bar and 300 K, respectively. The performed fit gives $K_0 = 29.3(2.7)$ GPa, $K_0' = 4$ (fixed), and $V_0 = 94.2(1.4)$ Å^3 for pressure range 0–15 GPa [Fig. 4(b)].

The intermediate pressure phase. At 17 GPa appreciable asymmetric broadening of the (100), (110), (201), and of some other diffraction peaks are observed. At this pressure a good quality fit could be obtained assuming a coexistence of two *iso*-symmetrical phases albeit with different atomic parameters [see Fig. 3(b)].[23] One of the phases is identified as the original LP and the other as a new, designated as *intermediate* pressure (IP) phase with larger c and reduced a parameters [Fig. 4(a)]. The c/a value exhibits a discontinuous $\sim 5\%$ increase at the LP→IP transition and attains a value of 1.67 the same as for ambient pressure. Both LP and IP phases have practically the same crystal volume and iodine coordinates as can be verified from Fig. 4(b) and Table I. The combined $V(P)$ data for both phases could be fitted with a single Birch-Murnaghan equation using $K_0 = 23.2(2.1)$ GPa, $K_0' = 4$ (fixed), and $V_0 = 97.4(1.9)$ Å^3.

The high pressure phase. The diffraction pattern obtained at ~ 20 GPa shows a significant splitting of the diffraction peaks indicative of the formation of a new high-pressure modification (HP) [Fig. 2(a)]. This new phase coexists with the IP phase [Fig. 3(c)] and its relative abundance, based on the GSAS fitting, increases sluggishly with rising pressure, reaching 100% at ~ 35 GPa. Except for the pattern corresponding to the original CdI_2 type structure, some ''additional'' weak peaks characterize the HP phase [particularly peaks indexed as (112), (113) on Fig. 2]. It is possible to interpret the HP diffraction data within the same CdI_2 structure by adopting the big cell (BC) model. This model allows (i) the formation of a new Fe sublattice assuming that a quarter of the Fe atoms are displaced towards the former (Fe-free) I-I interlayer sites [Fig. 1(b)] and (ii) the doubling of all lattice parameters. The result of a refinement applying the BC model for 27.5 GPa is shown in Fig. 3(c) and that obtained in the 20–35 GPa range is summarized in Fig. 4 and Table II.[24] The pressure dependence of the lattice parameters and volume depicted in this figure were calculated per formula unit to allow the comparison of the HP data with those of the LP and IP phases. One can see that the transition to the HP phase is accompanied by a significant and discontinuous reduction of volume ($\sim 5\%$) and c ($\sim 9\%$), as well by a slight increase of a while the c/a ratio dropped by $\sim 10\%$ [see Figs. 4(a), 4(b)]. The $V(P)$ data for the HP phase can well be described by a Birch-Murnaghan equation[21] (1) which yields the following values $K_0 = 63(2)$ GPa, $K_0' = 4$ (fixed), and $V_0 = 74.95(48)$ Å^3.

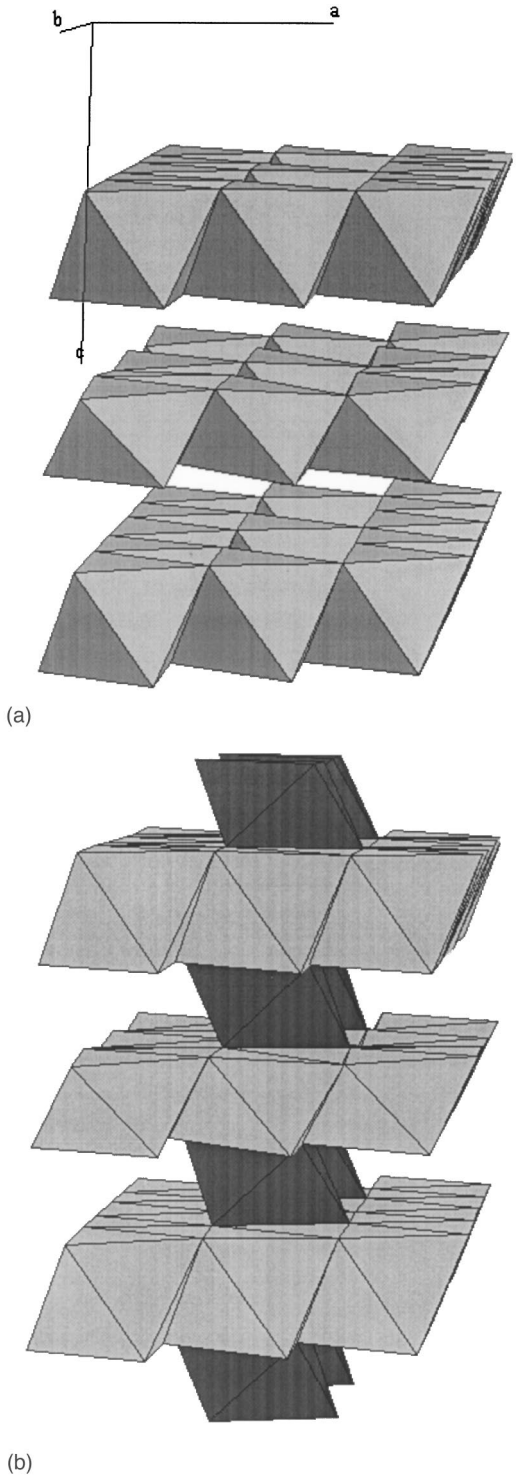

FIG. 1. (a) Polyhedral representation of the CdI_2-type crystal structure of FeI_2 up to ~20 GPa. The crystal is formed of intralayer covalently bonded I-Fe-I held together by I-I interlayer Van der Waal's forces. (b) Polyhedral representation of proposed HP FeI_2 structure of the BC type. According to this model a quarter of the Fe positions are transferred to the former free I-I interlayer positions. Note that if the dark octahedra were absent the structure would have been identical to the low-pressure, CdI_2 type.

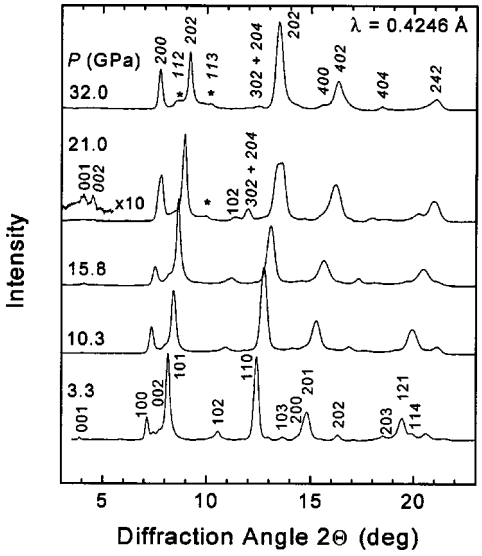

FIG. 2. X-ray powder diffraction patterns of FeI_2 at $T=298$ K at various pressures. Note the distinctive splitting of the diffraction peaks at 21 GPa, especially the (001), (102). A part of the spectrum in the 2θ range of $3°-5.5°$ is shown in $\times 10$ magnification to emphasize the (001) splitting. Weak peaks, which appear at 20 GPa in addition to the original CdI_2 type structure ones, are marked with an asterisk. Italics correspond to the diffraction peaks of the HP phase.

With pressure increase to ~35 GPa the ''additional'' weak peaks [Fig. 2(a)] start to disappear gradually and for $P>40$ GPa the best-fit could be obtained assuming the CdI_2-type structure [Fig. 3(d), Table I]. This signals the onset of a structural transformation resulting in a domination of the CdI_2 type phase on the range 40–70 GPa. This transformation does not carry any appreciable volume change and the $V(P)$ data, up to and beyond 40 GPa, could be fitted with a Birch-Murnaghan equation for the 20–70 GPa whole pressure range. It is noteworthy that this transformation was not accompanied by any apparent hysteresis.

IV. DISCUSSION AND CONCLUSIONS

We carried out total energy calculations for FeI_2 for two different types of structures, the CdI_2 type (SC) and the BC model-type (BC) [see Fig. 5(a)]. The numerical results of the calculations for fully relaxed c/a and internal parameters are summarized in Tables III and IV for SC and BC structures, respectively.[25] Calculations employing the GGA method imply a SC→BC transition taking place at $V/V_0 \sim 0.72$. At the reduced volume range 0.72–0.67, the total energy value for BC is lower than that of the SC thereby favoring the BC. A reverse BC→SC transformation takes place at $V/V_0 \sim 0.67$. Thus, our *ab initio* calculations support the experimental finding of the BC-type phase and the SC↔BC transitions. The V/V_0 calculated transitions are somewhat different than the experimental ones occurring at 0.7 and 0.58. But taking into account the limitations of the theoretical calculation, which assumes only fully ordered structures at $T=0$, the comparison with the experimental data looks rather good (see also Ref. 29). Furthermore, the SC→BC transition agrees with our predicted collapse of magnetic moments

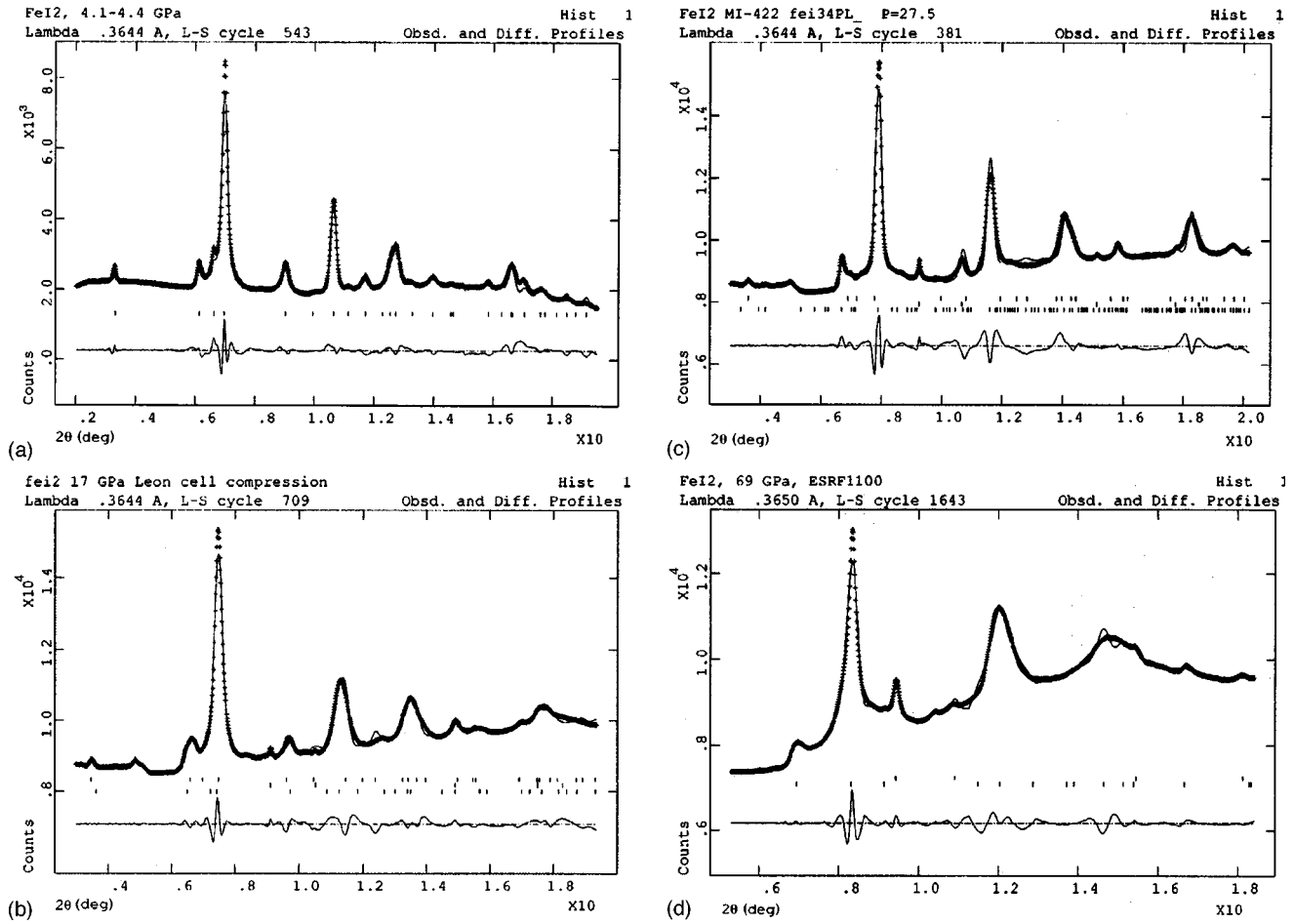

FIG. 3. Typical examples of analyzed integrated patterns collected at (a) 4.2 GPa, assuming a CdI_2-type structure for the LP phase, (b) 17 GPa (LP: lower ticks, Au markers: middle ticks, IP: upper ticks), (c) 27.5 GPa (HP: lower ticks, Au markers: middle ticks, IP: upper ticks) and assuming a BC model for HP phase, and, (d) 69 GPa, assuming a CdI_2-type structure for HP phase. The GSAS program package was used.

[Fig. 5(b)].[26] This is in good agreement with MS experimental observations discussed below.

In addition to the structural transformations predicted from the *ab initio* calculations, a new phenomenon revealed in our experiment is the LP→IP phase transition starting at 17 GPa. It is noteworthy that according to ^{57}Fe MS data (Ref. 10) a quenching of the orbital term occurs at 17 GPa resulting in breakdown of the spin-orbit coupling and reorientation of the magnetic moment. Both transitions, the crystallographic LP→IP and the quenching of the orbit term of the moment caused by the enhanced crystal field, emerge at the same pressure range without any detected volume nor isomer shift (IS)[27] changes, that would have implied a first-order phase transition. Is the crystallographic observation of the LP→IP transition related to quenching of the orbital term? Perhaps yes. Contribution to the form and energy of the atomic interactions resulting from spin-orbit terms could be significant,[28] hence we propose that the observed lattice distortion in the *c* direction, at the IP phase, could be attributed to the orbital quenching.

The observed transition starting at 20 GPa is in accordance with the SC→BC transition obtained from our *ab initio* calculation. Both are attributed to structural modification from the original CdI_2 type structure to the BC model type. However it should be emphasized that the calculations do not imply a significant volume decrease as experimentally observed.[29] The BC transition by itself is not sufficient to explain the large volume decrease; fundamental electronic processes must take place to explain that. A possible indication of such a process obtained from our *ab initio* calculations is the magnetic moments collapse. And indeed the MS and resistance results[10] corroborate this theoretical prediction through the observation of a Mott transition. The abundance of the diamagnetic/metallic phase increases with rising pressure to reach 100% at ~35 GPa similar to the abundance of the HP structural modification as deduced from the XRD data. Hence the transition starting at 20 GPa is a complex transformation including a Mott transition concurrent with the structural phase transition.

The transition from CdI_2 to the BC model structure is an isostructural transition consisting in a displacement of a quarter of the Fe positions towards the former Fe-free I-I interlayer sites. In fact this transition may indicate a trend of the Fe sites to disorder in the new HP phase. It could be proposed that the breakdown of the *d*-electrons may enhance

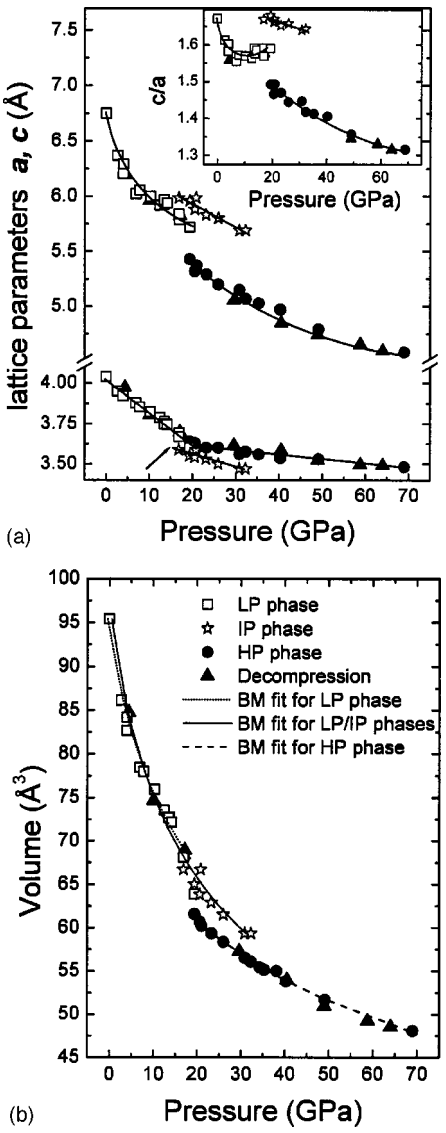

FIG. 4. Pressure evolution of the FeI_2 cell dimensions: (a) unit cell parameters [for symbols see (b)]. The transition to the HP phase is accompanied by ~9% reduction of c. Note the peculiarities in parameters behavior corroborated with the quenching of the orbital term at $P \sim 17$ GPa (arrow). The inset shows a variation of c/a with pressure in the LP, IP, and HP phases. Solid lines are to guide the eyes. (b) Unit cell volume. The (●●●), (——), and (– – –) lines are theoretical fits for the LP, LP+IP, and HP phases, respectively, using the Birch-Murnaghan equation of state. The transition to the HP phase is accompanied by ~5% volume reduction.

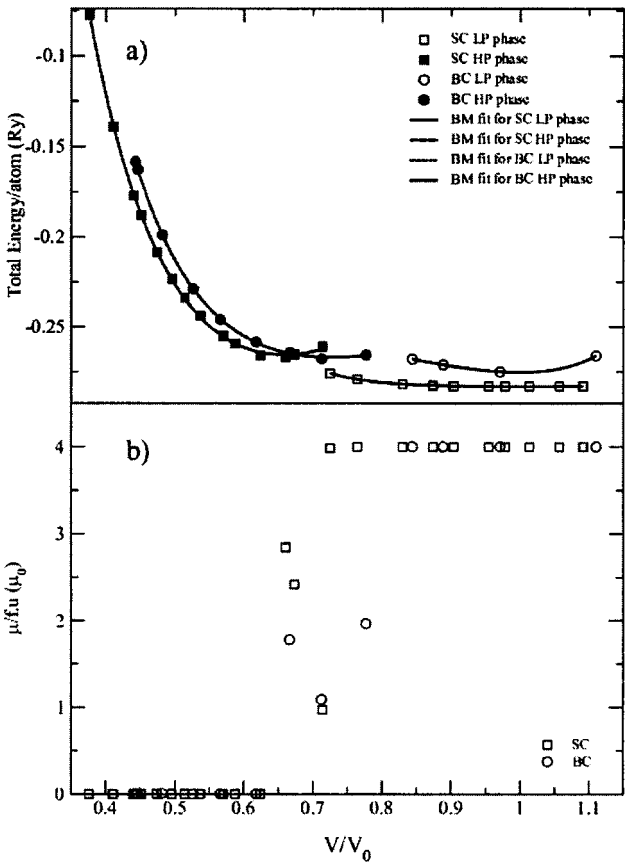

FIG. 5. (a) The calculated total energy of CdI_2-type and BC-type structures of FeI_2 as a function of reduced volume. (b) The magnetic moment as a function of reduced volume for CdI_2 and BC structures obtained by FP-LMTO (GGA) simulations. One can clearly distinguish two regions: the low and high pressure (LP, HP) regimes corresponding to high and low spin states, respectively. The (——), (– – –), (●●●), and (●-●) lines are Birch-Murnaghan fits for the SC-LP, SC-HP, BC-LP, and BC-HP phases, respectively.

this trend. The reversal transition is observed upon a further pressure increase in accordance with BC→SC transition obtained at the *ab initio* calculations. This transformation is caused by the switch-back of the Fe atom to its former I-I intralayer sites and resulting in the ordered CdI_2-type phase for pressures above 40 GPa.

As it was mentioned above the significant alterations of the lattice parameters and volume, associated with the transition to HP phase, are conditioned by the Mott transition starting at 20 GPa. We have attempted to identify a mechanism of the Mott transition [Mott-Hubbard or charge-transfer (CT) type[1,30]] from an analysis of interatomic distances variations through the transition. Such analysis (see Fig. 6) shows that up to ~20 GPa the main reason for the shortening of the c-parameter with rising pressure is the reduction in the interlayer I-I distances while the intralayer I-I distances hardly change. At ~20 GPa a significant decrease in the Fe-I bond lengths is observed resulting in shortening of the intralayer I-I distances. This Fe-I bond lengths shrinkage is responsible for the abrupt change of the c-axis length and consequently of the volume. The substantial reduction in Fe-I bond lengths with minimal changes in the Fe-Fe distances suggest that the iodine p bands play an important role in the insulator-metal transition. This prompts us to elect the mechanism of the correlation breakdown as the CT gap closure, e.g., the pressure-induced overlap of I $5p$ band with the Fe-$3d$ upper band.

In contrast to the NiI_2 layered system the pressure-induced first-order MT in FeI_2 is a sluggish process, namely, the abundance of the diamagnetic/metallic HP phase which concurs with a significantly reduced volume, increases gradually with pressure and is fully transformed at $P \sim 35$ GPa. It should be pointed out that according to prelimi-

TABLE III. The calculated structural parameters obtained by FP-LMTO (GGA) simulations for CdI_2-type structure at various crystal volumes.

V/V_0	a (Å)	c/a	u
0.376	3.36637	1.24468	0.2735
0.410	3.44546	1.26624	0.2705
0.440	3.51098	1.28251	0.2680
0.451	3.53005	1.29225	0.2670
0.4741	3.57269	1.31151	0.2639
0.495	3.60473	1.33424	0.2610
0.514	3.63014	1.35556	0.2586
0.536	3.66169	1.37826	0.2560
0.570	3.70233	1.41737	0.2512
0.587	3.72448	1.43396	0.2487
0.624	3.76922	1.47020	0.2425
0.660	3.68941	1.65933	0.2650
0.673	3.71437	1.65752	0.2632
0.713	3.77975	1.66701	0.2584
0.725	3.79024	1.67936	0.2567
0.764	3.86424	1.67028	0.2518
0.830	3.93129	1.72260	0.2402
0.873	3.98392	1.74236	0.2328
0.899	3.99556	1.78675	0.2269
0.952	4.001667	1.87866	0.2151
0.978	3.99868	1.92990	0.2116
1.013	4.00183	1.99411	0.2030
1.057	4.01356	2.06187	0.1949
1.092	4.01238	2.13192	0.1883

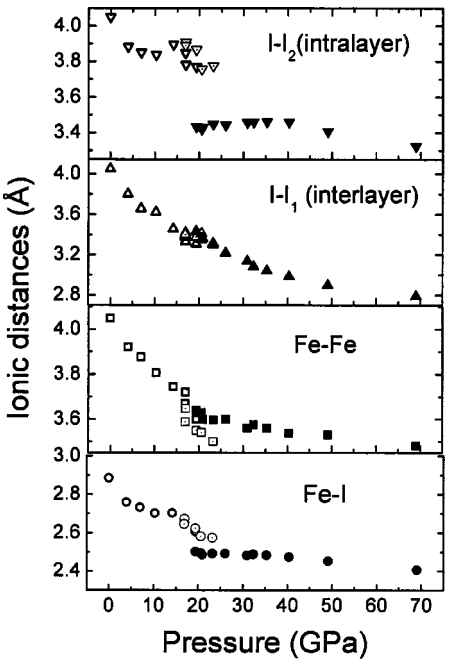

FIG. 6. Pressure evolution of the interatomic distances. Open, dot center, and solid symbols correspond to the LP, IP, and HP phases, respectively. One can see from this figure and Table I that in the LP and IP phases the Fe-I intralayer distances do indeed decrease with pressure but not so fast as the c parameter. In other words, the pressure primarily reduces the empty space between the I-Fe-I layers, leaving the layer itself rather rigid. At the IP→HP transition a discontinuous decrease of the Fe-I bond lengths is observed resulting in the shortening of the intralayer I-I distances.

nary data some of the structural alterations in accordance with the Mott transition could be related also to the ''classical'' NiI_2 system. It might be that as a rule a Mott transition coincides with a structural phase transition resulting sometimes in a sluggish and sometimes in an abrupt process, depending obviously on the extent of the volume collapse. The latter could be related to a mechanism of the transition (MH or CT type).

Thus up to ~17 GPa the crystal structure of FeI_2 can be assigned to the low-pressure CdI_2-type phase with a continuous decrease of crystal volume due to the increase of the pressure. At 17 GPa an onset of the structurally identical intermediate pressure phase is observed albeit with different atomic parameters. We attribute the LP-IP structural transition as a result of the sudden quenching of the orbital-term resulting in the breakdown of the spin-orbit coupling. At 20

TABLE IV. The calculated structural parameters obtained by FP-LMTO (GGA) simulations for BC model-type structure at various crystal volumes.

V/V_0	a	c/a	$Fe_{1(z)}$	$I_{1(z)}$	$I_{2(z)}$	$I_{3(x)}$	$I_{3(z)}$	$I_{4(x)}$	$I_{4(z)}$
0.442	6.85906	1.36044	0.2509	0.3629	0.8647	0.1696	0.1286	0.1705	0.6295
0.446	6.85402	1.37412	0.2530	0.3640	0.8651	0.1698	0.1291	0.1710	0.6283
0.482	6.97747	1.40650	0.2498	0.3682	0.8686	0.1705	0.1293	0.1709	0.6297
0.526	7.11736	1.44762	0.2505	0.3730	0.8731	0.1715	0.1301	0.1717	0.6300
0.565	7.21475	1.49359	0.2488	0.3773	0.8772	0.1720	0.1302	0.1721	0.6303
0.617	7.42538	1.49683	0.2561	0.3800	0.8810	0.1720	0.1271	0.1731	0.6263
0.666	7.53006	1.54818	0.2380	0.3704	0.8846	0.1724	0.1211	0.1680	0.6343
0.712	7.71184	1.54119	0.2379	0.3731	0.8886	0.1729	0.1183	0.1689	0.6350
0.776	7.84208	1.59762	0.2524	0.3769	0.8776	0.1686	0.1281	0.1685	0.6278
0.844	8.05465	1.60228	0.2513	0.3839	0.8840	0.1683	0.1270	0.1685	0.6269
0.888	8.18796	1.60557	0.2519	0.3896	0.8895	0.1677	0.1259	0.1676	0.6262
0.970	8.38178	1.63549	0.2335	0.3945	0.9023	0.1665	0.1253	0.1681	0.6216
1.110	9.03540	1.49357	0.2133	0.3925	0.9374	0.1553	0.1313	0.1798	0.6122

GPa, in concert with the MT, significant alterations of the lattice parameters, and crystal volume take place. High-pressure diffraction data could be interpreted using a model which within the same CdI_2-type structure a formation of a new Fe sublattice and doubling of lattice parameters takes place. This transformation of the Fe sublattice may signify a trend of the Fe sites to disorder in the new HP phase. The substantial reduction in the Fe-I bond lengths with minimal changes in the Fe-Fe distances at the transition suggests that the iodine *p* bands play an important role in the IMT. This allows us to categorize the gap as of a charge-transfer type. The pressure-induced first-order MT in FeI_2 is a sluggish process, namely, the abundance of the metallic nonmagnetic HP phase characterized by a significantly reduced volume, increases gradually with pressure and is fully transformed at $\sim$35 GPa. With further pressure increase a reverse trend to an ordering of the Fe positions is observed resulting in the onset of the CdI_2-type structure. The experimental results are in good agreement with the *ab initio* calculations. Finally, the present studies reveal two effects which have not been reported before, namely, a substantial change of the lattice parameters corroborating the idea of quenching of the orbital moments and an indication of Fe-sublattice disorder concurrent with correlation breakdown.

ACKNOWLEDGMENTS

This research was supported in parts by BSF Grant No. 9800003, and by Israeli Science Foundation Grant No. 2000-36. We are grateful to Dr. G. R. Hearne for his useful comments.

[1] N. F. Mott, *Metal-Insulator Transitions* (Taylor & Francis, London, 1990), and references therein.

[2] M. P. Pasternak and R. D. Taylor, Hyperfine Interact. **47**, 415 (1989); **128**, 81 (2000).

[3] G. Kh. Rozenberg, G. R. Hearne, M. P. Pasternak, P. Metcalf, and J. M. Honig, Phys. Rev. B **53**, 6482 (1996).

[4] M. P. Pasternak, R. D. Taylor, A. Chen, C. Meade, L. M. Falicov, A. Giesekus, R. Jeanloz, and P. Y. Yu, Phys. Rev. Lett. **65**, 790 (1990).

[5] M. P. Pasternak, R. D. Taylor, and R. Jeanloz, J. Appl. Phys. **70**, 5956 (1991); M. P. Pasternak, R. D. Taylor, and R. Jeanloz, in *Frontiers of High-Pressure Research*, edited by H. D. Hochheimer and R. D. Etters (Plenum, New York, 1991), p. 227.

[6] J. L. García-Muñoz, J. Rodríguez-Carvajal, P. Lacorre, and J. B. Torrance, Phys. Rev. B **46**, 4414 (1992).

[7] P. D. Dernier and M. Marezio, Phys. Rev. B **2**, 3771 (1970).

[8] G. Kh. Rozenberg, L. S. Dubrovinsky, M. P. Pasternak, O. Naaman, T. Le Bihan, and R. Ahuja, Phys. Rev. B **65**, 064112 (2002).

[9] I. Loa, P. Adler, A. Grzechnik, K. Syassen, U. Schwarz, M. Hanfland, G. Kh. Rozenberg, P. Gorodetsky, and M. Pasternak, Phys. Rev. Lett. **87**, 125501 (2001).

[10] M. P. Pasternak, W. M. Xu, G. Kh. Rozenberg, R. D. Taylor, G. R. Hearne, and E. Sterer, Phys. Rev. B **65**, 035106 (2002).

[11] R. W. G. Wycoff, *Crystal Structures* (Interscience, New York, 1981), Vol. 1.

[12] Pure elemental I_2 was prepared on the same evacuated tube by thermal dissociation of spectroscopic pure PdI_2 at 300 °C.

[13] E. Sterer, M. P. Pasternak, and R. D. Taylor, Rev. Sci. Instrum. **61**, 1117 (1990).

[14] A. P. Hammersley, S. O. Svensson, M. Hanfland, A. N. Fitch, and D. Hausermann, High Press. Res. **14**, 235 (1996).

[15] A. C. Larson and R. B. Von Dreele (unpublished).

[16] J. M. Wills, O. Eriksson, M. Alouani, and D. L. Price, in *Electronic Structure and Physical Properties of Solids*, edited by H. Dressey (Springer Verlag, Berlin, 2000), p. 148; J. M. Wills and B. R. Cooper, Phys. Rev. B **36**, 3809 (1987); D. L. Price and B. R. Cooper, *ibid.* **39**, 4945 (1989).

[17] J. P. Perdew, K. Burke, and M. Ernzerhof, Phys. Rev. Lett. **77**, 3865 (1996).

[18] R. Ahuja, J. Wills, B. Johansson, and O. Eriksson, Phys. Rev. B **48**, 16 269 (1993).

[19] O. K. Andersen, Phys. Rev. B **12**, 3060 (1975).

[20] H. L. Skriver, *The LMTO Method* (Springer, Berlin, 1984).

[21] D. J. Chadi and M. L. Cohen, Phys. Rev. B **8**, 5747 (1973); S. Froyen, *ibid.* **39**, 3168 (1989).

[22] O. L. Anderson, *Equations of State of Solids for Geophysics and Ceramic Science* (Oxford University Press, Oxford, 1995).

[23] A worse quality fit could be obtained if one assumes the existence of only one CdI_2 type phase. But even for this case the calculated lattice parameters and c/a ratio will be close to that obtained for the IP phase and their pressure dependencies will be similar to the presented above [Figs. 4(a), 4(b)].

[24] There are eight internal refined structural parameters for the BC phase. It is difficult to expect that high-pressure XRD data could provide sufficient information for unambiguous refinements for all of them, especially in the two-phase region. Therefore, the refinement for this phase was performed with fixed I_1 and I_2 positions (multiplicity 2), $I_{1(z)}=0.375$, $I_{2(z)}=0.875$, and free I_3, I_4 positions (multiplicity 6). Such a full-profile fit comes out to be stable and standard errors of refined coordinates (maximum 0.015 in the *z* coordinates of I atoms) reasonably low, which allow us to discuss the general trend of the structural variations of FeI_2 under pressure.

[25] Our calculations confirm the general trend of the iodine coordinate *u* to increase with pressure as observed experimentally. The calculated $c/a(V/V_0)$ flattens at the vicinity of the LP$\rightarrow$HP phase transition followed by a substantial drop at the transition.

[26] At $V/V_0 \leqslant 0.72$ the low spin state starts to be a stable solution for both SC and BC structures and at $V/V_0 \leqslant 0.63$ the magnetic moment drops to zero. Because the low- and high-spin solutions have local minima [see Fig. 5(a)] it is not possible to fit with one Birch-Murnaghan equation of state (BMEOS) function for both regions. Similar to the experiment two different BMEOS's were obtained for the LP and HP pressure regimes. The BMEOS function and its fitted parameters in the SC-HP calculated phase agreed well with the experimental points resulting in K_0

$=70.8(2)$ GPa, $K_0'=4$ (fixed), and $V_0=72.50(4)$ Å^3. However, the theoretical bulk modulus $K_0=3$ GPa of the SC-LP phase significantly differs from that calculated from the experimental data. It is possible that this disagreement is due to the fact that the LP phase calculation a ferromagnetic solution was used instead of an antiferromagnetic one. For the SC-HP phase magnetism is not present at all which explains the good agreement between theory and experiment.

[27] A drop in the IS in ^{57}Fe, which is negatively proportional to the increase in the *s*-electron density at the Fe nucleus, follows usually a volume reduction (see Ref. 2).

[28] J. C. Slater, *Quantum Theory of Molecules and Solids* (McGraw-Hill, New York, 1963), Vol. 1.

[29] The calculation procedures show a decrease of the effective pressures instead of volume drop. The reason being that it's not a variable in this model: We calculate total energy and magnetic moment at through the second derivative of energy with respect to volume which produces pressure values. Such a procedure does not allow the calculation of volume changes which could be associated with the magnetic moment collapse.

[30] J. Zaanen, G. A. Sawatzky, and J. W. Allen, Phys. Rev. Lett. **55**, 418 (1985).